Supplemental Figure Legends

Supplemental Figure 1 related to Figures 2 and 3. Naive and memory *Vhl*$^{fl/fl}$*dLck-cre* cells rely on glycolytic metabolism following *in vitro* stimulation. (**A**) Schematic of experimental design for all *in vivo* experiments; 1 x 10^4 WT or *Vhl*$^{fl/fl}$*dLck-cre* cells were adoptively transferred i.v. into naive hosts with differential expression of congenic CD45 alleles followed by infection one day later with LCMV Armstrong. (**B**) Analysis of proliferation of sort-purified memory WT and *Vhl*$^{fl/fl}$*dLck-cre* cells 72 hours following restimulation with irradiated peptide pulsed splenocytes. (**C**) SRC of *in vitro* activated WT and *Vhl*$^{fl/fl}$*dLck-cre* cells cultured with IL-2 or IL-15. (**D**) Analysis of proliferation 48 hrs following *in vitro* activation with anti-CD3 and anti-CD28 of enriched polyclonal WT and *Vhl*$^{fl/fl}$*dLck-cre* CD8$^+$ T cells from spleen by dilution of Cell Trace Violet. (**E**) Relevant intracellular metabolites of *in vitro* activated and expanded *Vhl*$^{fl/fl}$*dLck-cre* and WT CD8$^+$ T cells analyzed by metabolomics performed by Metabolon. Fold change (FC) is comparison of *Vhl*$^{fl/fl}$*dLck-cre* over WT ($p \leq 0.05$ for all FC indicated). Critical metabolic enzymes regulating pyruvate usage following glycolysis listed (HIF regulated in red with FC from gene expression analysis).

Supplemental Figure 2 related to Figure 4. Accelerated memory precursor cell differentiation of *Vhl*$^{fl/fl}$*dLck-cre* cells is primarily cell intrinsic. (**A**) Kinetic analysis of *Vhl*$^{fl/fl}$*dLck-cre* and WT donor P14 CD8$^+$ T cells from PBL following mixed transfer (1:1) of 10^4 cells into congenically distinct hosts and subsequent infection with LCMV by flow cytometry for expression of KLRG1 and CD127. (**B-C**) Flow cytometry analysis of phosphorylated S6 in WT and *Vhl*$^{fl/fl}$*dLck-cre* donor CD8$^+$ T cells in spleen during expansion (**B**) and at memory (**C**) following acute LCMV infection. (**C**) Splenocytes were pulsed with 1 μM gp33 prior to analysis. (**D-E**) Kinetic analysis of WT and *Vhl*$^{fl/fl}$*Hif1a*$^{fl/fl}$*Epas1*$^{fl/fl}$*dLck-cre* donor P14 CD8$^+$ T cells from

spleen following adoptive transfer and subsequent infection with LCMV by flow cytometry of KLRG1, CD127, and GzmB. (**D**) Representative flow cytometry analysis of KLRG1 and CD127 expression by WT and *Vhl*$^{fl/fl}$*Hif1a*$^{fl/fl}$*Epas1*$^{fl/fl}$*dLck-cre* donor P14 CD8^{+} T cells (left) at indicated time points and formation of terminal effectors compared to *Vhl*$^{fl/fl}$*dLck-cre* donor P14 CD8^{+} T cells relative to WT terminal effector formation. (**E**) Comparison of GzmB expression at indicated time points following acute viral infection by *Vhl*$^{fl/fl}$*Hif1a*$^{fl/fl}$*Epas1*$^{fl/fl}$*dLck-cre* to *Vhl*$^{fl/fl}$*dLck-cre* donor P14 CD8^{+} T cells relative to WT GzmB expression. (**F**) Percentage of indicated donor cells incorporating BrdU on day 6 of LCMV infection. Data in (**B-F**) show mean ± SEM with one-way ANOVA followed by Tukey's Multiple Comparison Test, ns $p > 0.05$, * $p < 0.05$, ** $p < 0.01$, ** $p < 0.001$.

Supplemental Figure 3 related to Figure 4. Gene-expression analysis of WT and *Vhl*$^{fl/fl}$*dLck-cre* KLRG1^{lo} cells at day 7 following infection supports accelerated differentiation of *Vhl*$^{fl/fl}$*dLck-cre* memory precursor cells. 'Volcano plots' of the comparison of WT versus *Vhl*$^{fl/fl}$*dLck-cre* cells. Showing clusters of genes identified from (Best et al., 2013). Numbers in bottom left and right corners indicate number of genes in that region. (**A**) We previously identified temporally regulated gene expression patterns of pathogen-reactive CD8^{+} T cells that were parsed into 10 unbiased groups (Best et al., 2013). Showing cluster VII (highlighted in green, left) and VIII (highlighted in light green, right) -specific genes overlaid on comparison of total WT and *Vhl*$^{fl/fl}$*dLck-cre* cell gene-expression. (**B**) Fold changes versus p value for the cluster of genes expressed 1.5-fold higher in WT KLRG1^{hi} effector cells compared to WT KLRG1^{lo} cells shows a loss of expression of KLRG1^{hi} associated genes by *Vhl*$^{fl/fl}$*dLck-cre* cells.

Supplemental Experimental Procedures

Mice

Mice were bred and housed in specific pathogen-free conditions in accordance with the Institutional Animal Care and Use Guidelines of the University of California San Diego. The following *Hif1a*$^{fl/fl}$ (Ryan et al., 2000) and *Epas1*$^{fl/fl}$ (Gruber et al., 2007) mice were previously described and crossed to *Vhl*$^{fl/fl}$ mice expressing the P14 TCR transgene and distal Lck driven Cre recombinase to obtain mice with homozygous loxP-flanked alleles without Cre or hemizygous for Cre and expression of the P14 TCR transgene. All mice were backcrossed over ten generations to the C57BL/6 background.

***In vitro* stimulation**

Naive WT and *Vhl*$^{fl/fl}$*dLck-cre* cells were enriched via magnetic bead separation and labeled with Cell Trace Violet (Thermo Fisher, C34557) prior to activation with plate bound anti-CD3 (145 2C11) and soluble anti-CD28 (37.51) and culture with or without indicated metabolic inhibitors. Memory WT and *Vhl*$^{fl/fl}$*dLck-cre* cells were sort-purified from host mice that had been infected 60 days prior with LCMV Armstrong and then labeled with Cell Trace Violet. Memory cells were then cultured with irradiated splenocytes pulsed with 1 μM gp33 peptide with or without indicated metabolic inhibitors.

Metabolomics

Metabolomic experiments were performed by Metabolon Inc. using GC/MS and LC/MS/MS platforms for determination of intracellular metabolites. Samples were normalized for protein concentration measured by the Bradford assay and rescaled to set the median to 1. The minimum value was substituted for missing metabolite values.

Supplemental References

Best, J.A., Blair, D.A., Knell, J., Yang, E., Mayya, V., Doedens, A., Dustin, M.L., Goldrath, A.W., and Consortium, T.I.G.P. (2013). Transcriptional insights into the CD8+ T cell response to infection and memory T cell formation. Nature Immunology *14*, 404-412.

Gruber, M., Hu, C.-J., Johnson, R.S., Brown, E.J., Keith, B., and Simon, M.C. (2007). Acute postnatal ablation of Hif-2α results in anemia. Proceedings of the National Academy of Sciences *104*, 2301-2306.

Ryan, H.E., Poloni, M., McNulty, W., Elson, D., Gassmann, M., Arbeit, J.M., and Johnson, R.S. (2000). Hypoxia-inducible Factor-1α Is a Positive Factor in Solid Tumor Growth. Cancer Research *60*, 4010-4015.

Phan et al. Supplemental Figure 1

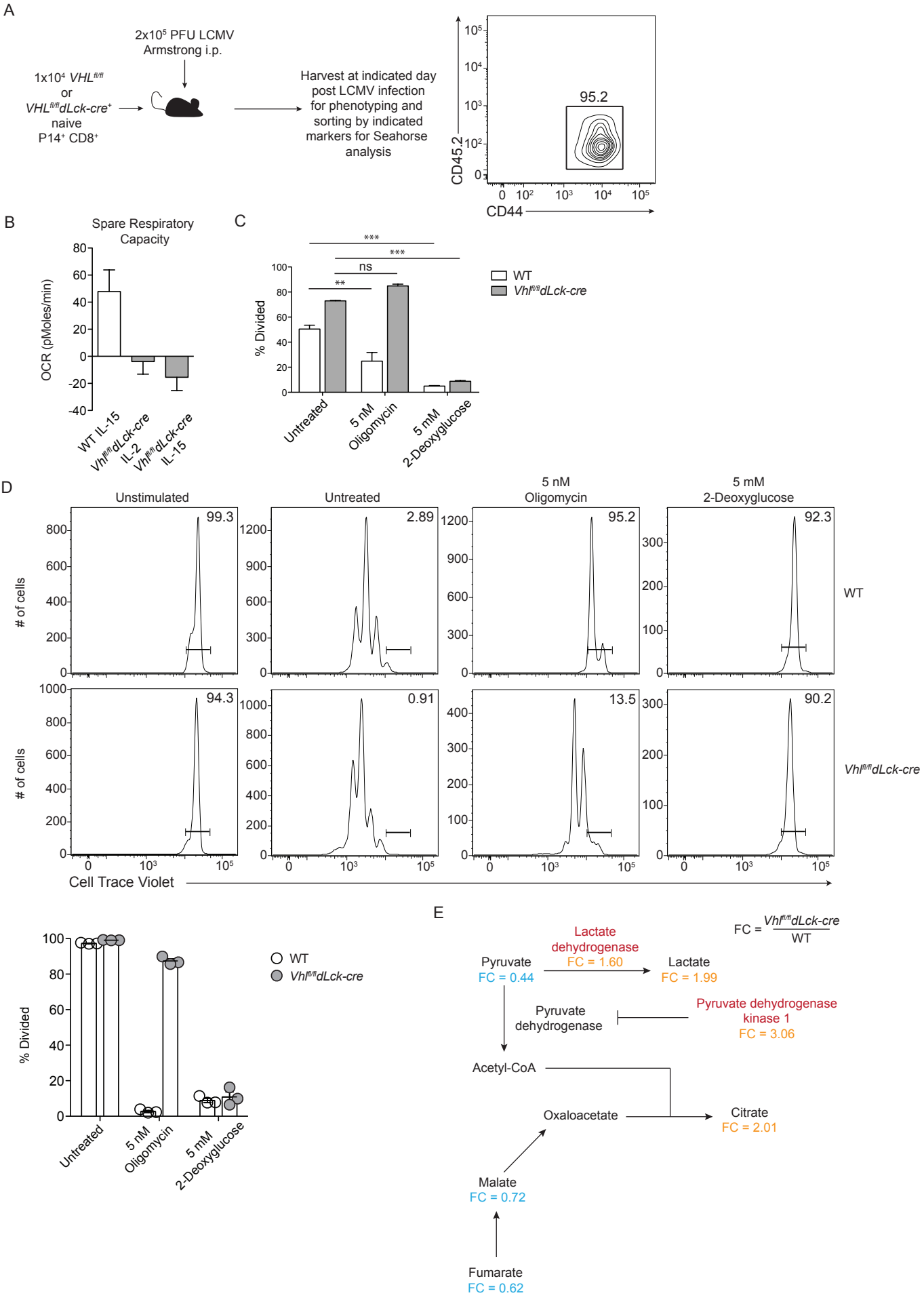

Phan et al. Supplemental Figure 2

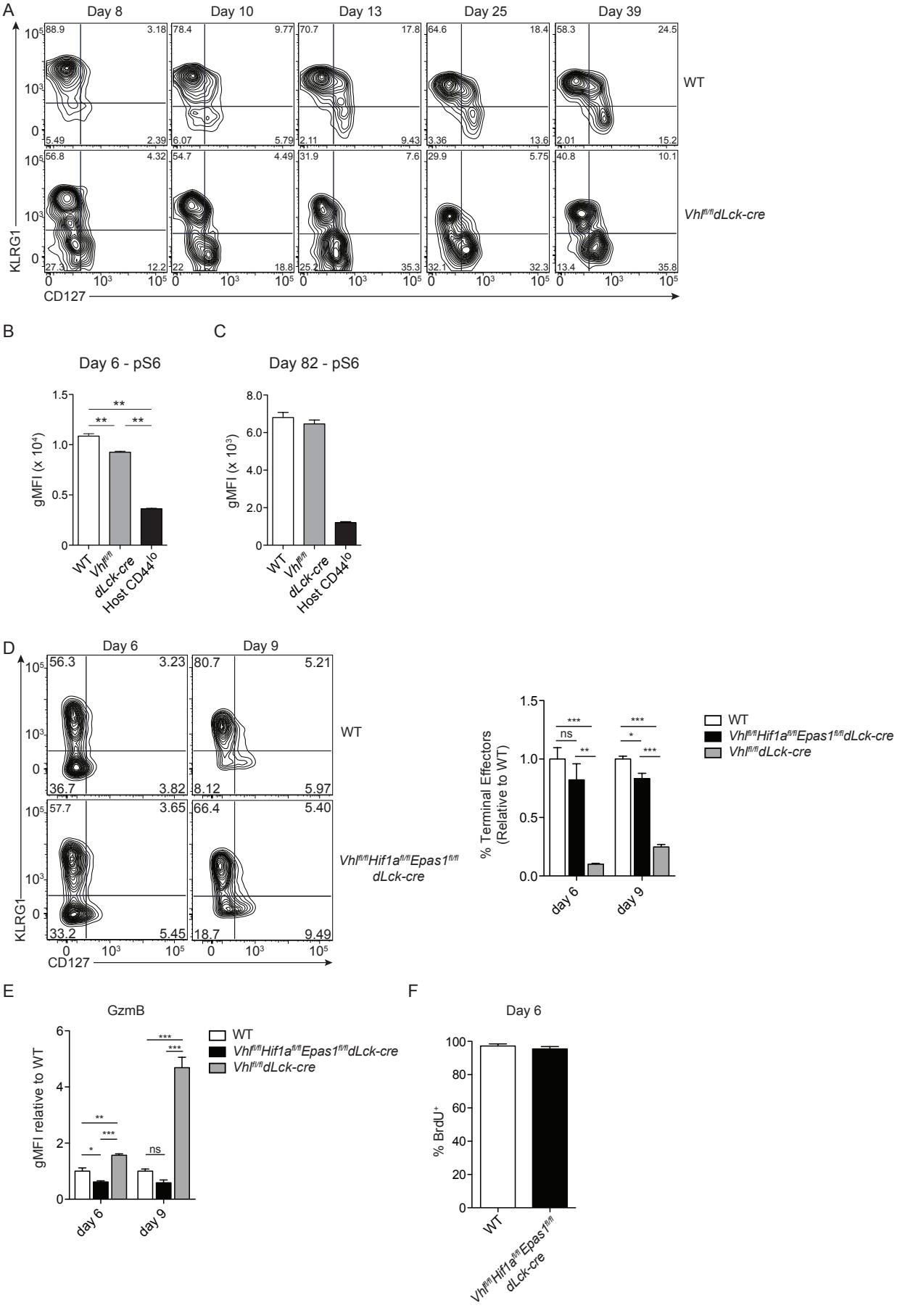

Phan et al. Supplemental Figure 3

A

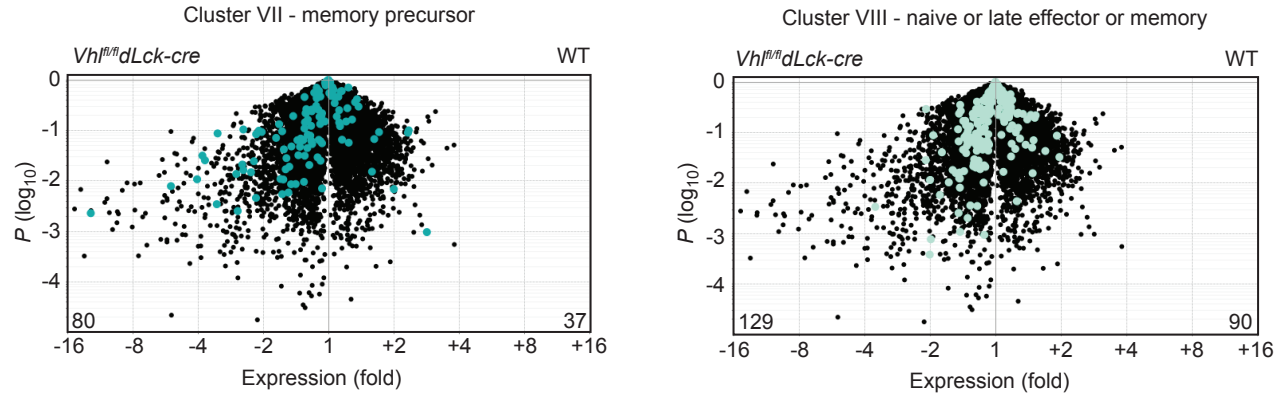

B